JACS Au
AN OPEN ACCESS JOURNAL OF THE AMERICAN CHEMICAL SOCIETY

pubs.acs.org/jacsau
Article

Highly Efficient Carbon Dioxide Electroreduction via DNA-Directed Catalyst Immobilization

Gang Fan, Nathan Corbin, Minju Chung,[§] Thomas M. Gill,[§] Evan B. Moore, Amruta A. Karbelkar, and Ariel L. Furst*

Cite This: *JACS Au* 2024, 4, 1413−1421
Read Online

ABSTRACT: Electrochemical reduction of carbon dioxide (CO_2) is a promising route to up-convert this industrial byproduct. However, to perform this reaction with a small-molecule catalyst, the catalyst must be proximal to an electrode surface. Efforts to immobilize molecular catalysts on electrodes have been stymied by the need to optimize the immobilization chemistries on a case-by-case basis. Taking inspiration from nature, we applied DNA as a molecular-scale "Velcro" to investigate the tethering of three porphyrin-based catalysts to electrodes. This tethering strategy improved both the stability of the catalysts and their Faradaic efficiencies (FEs). DNA-catalyst conjugates were immobilized on screen-printed carbon and carbon paper electrodes via DNA hybridization with nearly 100% efficiency. Following immobilization, a higher catalyst stability at relevant potentials is observed. Additionally, lower overpotentials are required for the generation of carbon monoxide (CO). Finally, high FE for CO generation was observed with the DNA-immobilized catalysts as compared to the unmodified small-molecule systems, as high as 79.1% FE for CO at −0.95 V vs SHE using a DNA-tethered catalyst. This work demonstrates the potential of DNA "Velcro" as a powerful strategy for catalyst immobilization. Here, we demonstrated improved catalytic characteristics of molecular catalysts for CO_2 valorization, but this strategy is anticipated to be generalizable to any reaction that proceeds in aqueous solutions.

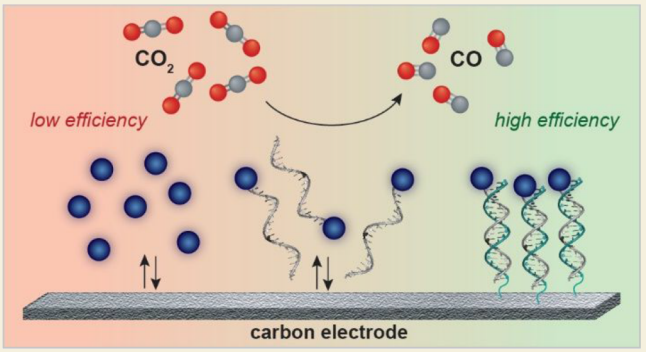

KEYWORDS: *Bio-inspired, catalysis, DNA "Velcro", electrochemical CO_2 reduction*

An expected 500 gigatons of carbon dioxide (CO_2) will be produced in the next five decades as a major byproduct of industrial processes.[1] Despite its abundance and potential as a one-carbon feedstock, CO_2 has yet to be extensively used to generate value-added chemicals.[2,3] The first step in this process is the reduction of CO_2 to generate carbon monoxide (CO), a key component of synthetic gas (syngas), which is used as a fuel source and as an intermediate for chemical production. Thus, significant effort has been devoted to the development of technologies to convert CO_2 to CO.[4−6] Electrochemical CO_2 reduction (CO_2 reduction reaction—CO_2RR) is one of the most common methods of CO_2 conversion, with many examples of both homogeneous and heterogeneous systems.[1,7,8] Small-molecule catalysts for CO_2RR are advantageous because of their tunability and well-defined active sites.[9−11] These catalysts can be employed homogeneously, but their immobilization on electrodes is advantageous,[12,13] as it reduces mass transport limitations and can improve catalyst−electrode interactions.[8] In heterogeneous systems, both the local environment surrounding the catalyst and the ability of the reactant to reach the active site significantly impact the conversion efficiency and reaction products.[14−16]

Synthetic catalysts promise tunability and scalability, but enzymes (native protein catalysts) often outperform these small molecules because of their substrate specificity and ability to both activate the reactant and stabilize the reaction intermediate.[17,18] Thus, there has been significant effort to improve synthetic catalysts by taking inspiration from biological systems.[19,20] One key active site found in many enzymes is porphyrin, a ligand structure that often chelates cobalt or iron (Figure 1a).[21] This moiety is found in enzymes ranging from oxygenases to peroxidases and is the core of engineered cytochromes capable of complex transformations including C−H activation.[21] Thus, we started from this biological molecule to improve CO_2RR. Using porphyrin-derived ligand structures, molecular catalysts have been shown

Received: December 24, 2023
Revised: March 3, 2024
Accepted: March 4, 2024
Published: March 25, 2024

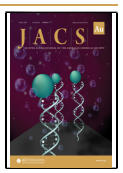

https://doi.org/10.1021/jacsau.3c00823
JACS Au 2024, 4, 1413−1421

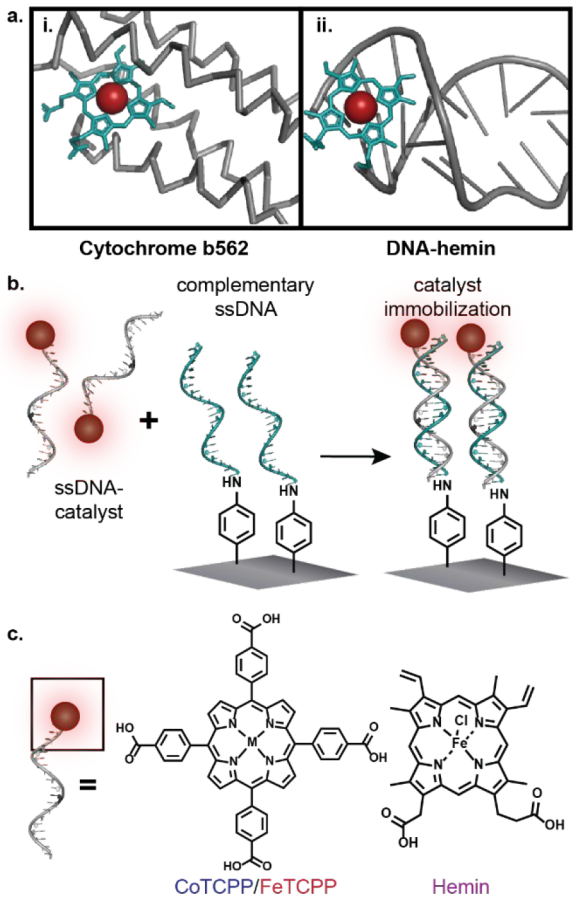

Figure 1. Bioinspired catalyst design. (a) Porphyrin catalysts in natural and engineered local environments. (i) Cytochrome b562 is a heme-containing protein thought to be involved in electron transport.[32] (ii) Hemin tethered to the terminus of one strand of DNA in a duplex for CO_2RR. (b) Catalyst immobilization using DNA "Velcro". Single-stranded DNA (ssDNA) conjugated to a small-molecule catalyst is hybridized to complementary DNA attached to a carbon electrode. (c) Small-molecule catalysts evaluated include Co(II) and Fe(III) tetrakis(4-carboxyphenyl)porphyrin (H_2TCPP)–CoTCPP, and FeTCPP, as well as hemin.

to perform CO_2RR, although their efficiency remains relatively low compared to other catalysts.[8]

One strategy to improve catalysis is to immobilize small molecules on electrode surfaces, either through direct grafting of a ligand to the electrode[14,22−26] or by noncovalent interactions between pyrene moieties appended to ligands and low-dimensional carbon surfaces.[27−29] However, these systems limit the conformational flexibility of the catalyst, constrain transport of the reactant to the catalytic center, are often limited by solubility, and yield current densities lower than their homogeneous equivalents.[30] We sought to improve heterogeneous catalysis with these small molecules using the chemical properties of DNA (Figure 1a); because of its stability, chemical tunability, and inherent self-recognition, DNA is an ideal material to serve as a generalizable platform for catalyst immobilization. The self-recognition of DNA, due to hydrogen bonding between proper base pairs, provides a sequence-specific, noncovalent adhesive mechanism for controlled surface attachment.[31] We therefore used DNA as a "molecular Velcro" to immobilize porphyrin-based CO_2RR catalysts.

DNA is often thought of solely in the context of the genetic code, but its three-dimensional structure imbues it with unique material properties beyond this role.[33−40] DNA is a naturally occurring polymer composed of two complementary oligonucleotide strands. These strands self-recognize through base-pair hydrogen bonding, serving as sequence-specific "Velcro". Further, once the DNA duplex is formed, the pi orbitals of the aromatic bases overlap to stabilize the structure of DNA.[41−43]

These properties have brought new opportunities in materials science,[34,36] sensing, and diagnostics.[44−46] Among them, DNA "Velcro" has been used to pattern cells[41,47−51] and antibodies.[31,34] Despite these advantages, DNA has not yet been applied to energy-relevant catalysis. Here, we demonstrate the first application of DNA "Velcro" to immobilize molecular CO_2RR catalysts on electrode surfaces (Figure 1b). The DNA-catalyst conjugates are readily synthesized and have improved stability as compared to the small-molecule catalysts alone simply through the incorporation of the DNA. Subsequent immobilization on carbon electrodes through hybridization to predeposited complementary DNA strands showed improved Faradaic efficiency (FE) toward CO production. We anticipate this method to be a general strategy to more easily and efficiently immobilize electrocatalysts for improved catalytic efficiency.

RESULTS AND DISCUSSION

Catalyst Selection and Synthesis

Based on their similarity to enzyme active sites, we selected three porphyrin-based catalysts for initial investigation (Co(II) and Fe(III) tetrakis(4-carboxyphenyl)porphyrin (H_2TCPP)–CoTCPP and FeTCPP, as well as hemin, Figure 1c). These catalysts all have known catalytic properties, a readily understood mechanism of proton-coupled electron transfer, and ability to vary the metal incorporated into porphyrin derivatives.[52] Iron-incorporated commercial hemin was used, and CoTCPP and FeTCPP were metalated with the corresponding metal ions from commercial H_2TCPP. Metalation was confirmed by mass spectrometry (Figure S1).

Synthesis and Optimization of DNA-Catalyst Conjugates

Although we took inspiration from enzyme active sites for the selection of catalysts, enzymes are often highly susceptible to deactivation from temperature fluctuations, pH changes, and the relative ionic strength of the solution in which they are maintained.[20] Further, proteins can be challenging to generate at scale without significant process optimization and costly purification.[53−55] Thus, to improve the stability and system control, we turned to another important biomolecule: DNA. Because DNA is highly stable under diverse aqueous conditions (a wide range of temperatures, pH's, and ionic strengths),[43] tunable, and synthetically tractable, it was an optimal choice as an addition to molecular catalysts that suffer from aqueous solubility issues and limited stability.

To investigate the impact of DNA on the CO_2RR with the porphyrin-based catalysts, we synthesized catalyst-oligonucleotide conjugates, which we term single-stranded DNA (ssDNA) conjugates. Traditional bioconjugation strategies were undertaken involving amide bond formation between the catalyst ligand containing carboxylic acids and amine-terminated ssDNA (Figure S2). Porphyrin-DNA conjugates were initially reported nearly three decades ago by Meunier and co-workers[56] and Hélène and co-workers[57] but have mainly

https://doi.org/10.1021/jacsau.3c00823
JACS Au 2024, 4, 1413−1421

been used in fundamental scientific studies (e.g., for DNA sensing[58] and interstrand cross-linking[59]). The relatively narrow range of applications to date is attributed to challenging synthesis, intermolecular interactions that can lead to aggregation, and solubility issues. Indeed, we initially chose the prevalent amide coupling conditions[60] (1-ethyl-3-(3-(dimethylamino)propyl)carbodiimide (EDC), 1-hydroxybenzotriazole (HOBt), and DIPEA) and found no noticeable conversion with any of the three molecular catalysts. We therefore evaluated a variety of prevalent reagents for amide bond formation and found that most of the established reagents resulted in very low yields for this reaction. The highest yields were consistently found with a combination of hexafluorophosphate azabenzotriazole tetramethyl uronium and *N*,*N*′-diisopropylethylamine (HATU/DIPEA) reagents, which provide decent conversion for all three ssDNA-catalyst conjugates. The matrix-assisted laser desorption/ionization time-of-flight (MALDI-TOF) mass spectrometry and reverse-phase high-performance liquid chromatography (RP-HPLC) confirmed the successful synthesis and purification of the hemin- and Co/FeTCPP-DNA conjugates (Figures S3 and S4).

Despite the prevalence of this reaction for bioconjugations and the similarity of the core ligand structures for the three catalysts evaluated, we observed significant differences in the efficacy of standard reagents based on the catalyst being conjugated. This observation is worth noting for the expansion of this technology to additional catalysts, as some optimization may be required for the coupling.

Carbon Surface Modification with DNA

Prior to surface immobilization of the ssDNA-catalyst conjugates, electrodes stably modified with complementary DNA were needed. Conventionally, electrode modification with biomolecules is performed on gold surfaces due to their ease of modification with any biomolecule containing a free thiol. Despite this ease, gold surfaces of sufficient quality for modification are costly, the accessible potential window is smaller than that of other materials, such as carbon, and the gold−thiol bond formed is relatively unstable and susceptible to reductive stripping. Thus, for the potentials required for CO_2RR, gold was an unsuitable material. We therefore developed and recently reported new chemistry to modify carbon electrodes with biomolecules using an oxidative coupling bioconjugation reaction (Figure 2a).[61]

Preparation of aniline-modified electrodes for DNA conjugation was achieved by electrochemically-induced grafting of *o*-nitroaniline through the generation of a diazonium salt and subsequent reduction of the resultant nitrobenzyl at the surface to an aniline moiety (Figure 2a). The successful electrode modification was confirmed by characteristic reductive peaks observed in the cyclic voltammogram (CV) (0.15 V vs SHE, and −0.7 V vs SHE, respectively; Figure S5). Subsequent coupling of ssDNA to aniline-modified screen-printed electrodes (SPEs) was accomplished using the mild oxidant ferricyanide and *o*-aminophenol-modified DNA (Figure S6).

Successful coupling was validated by hexammineruthenium (RuHex) DNA quantification. RuHex interacts electrostatically with the DNA backbone to act as a phosphate counter (Figures 2b and S7). From these results, the surface concentration of oligonucleotides was calculated to be $(7.2 \pm 3.0) \times 10^{-12}$ mol/cm^2 (Figure S7, detailed methods are described in SI).[62] This

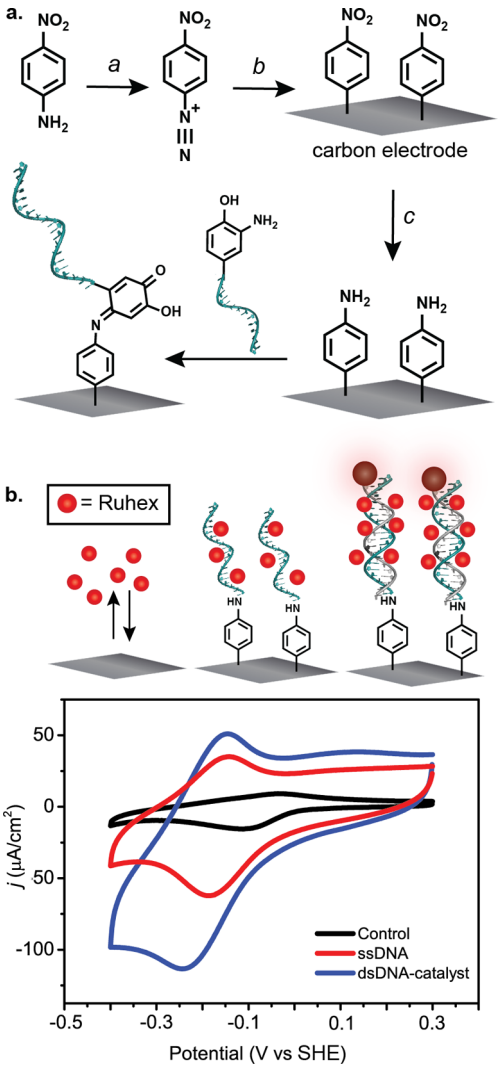

Figure 2. Carbon electrode modification with DNA. (a) A *p*-nitroaniline is used as a chemical handle for DNA attachment. To modify an electrode with anilines, an in situ diazonium is generated (a). Upon electrochemical reduction, a carbon−carbon bond is generated between the nitrobenzyl moiety and the electrode surface (b). Electrochemical reduction is again used to reduce the nitrobenzyl group to an aniline on the surface (c). Aminophenol-DNA is then directly tethered to the modified electrode. (b) ssDNA on the electrode is hybridized with complementary ssDNA-catalyst. The ruthenium ions interact electrostatically with the DNA backbone to act as a phosphate counter, resulting in a faradaic electrochemical signal. CV of catalyst-ssDNA-functionalized (blue), ssDNA modified (red), or uncoated (black) SPE in a stock solution (10 mM tris buffer, pH 7.4, containing 2 μM RuHex), carried out at a scan rate of 500 mV s^{-1}.

is well within the standard DNA coverages observed using conventional gold−thiol chemistries, which generally range from 1 to 100 pmol/cm^2.[42,43,63] Thus, the maximum surface density of catalyst loading on the electrode following hybridization is 7.2 pmol/cm^2. To evaluate the efficacy of this modification on more conventional substrates for catalyst immobilization, we performed the same protocol on carbon paper to add ssDNA to the surface. Just as with the SPEs, the successful carbon paper modification was confirmed by a reductive peak observed in the CV (0.1 V vs SHE, and −0.75 V vs SHE, respectively; Figure S8). After coupling of ssDNA to

https://doi.org/10.1021/jacsau.3c00823
JACS Au 2024, 4, 1413−1421

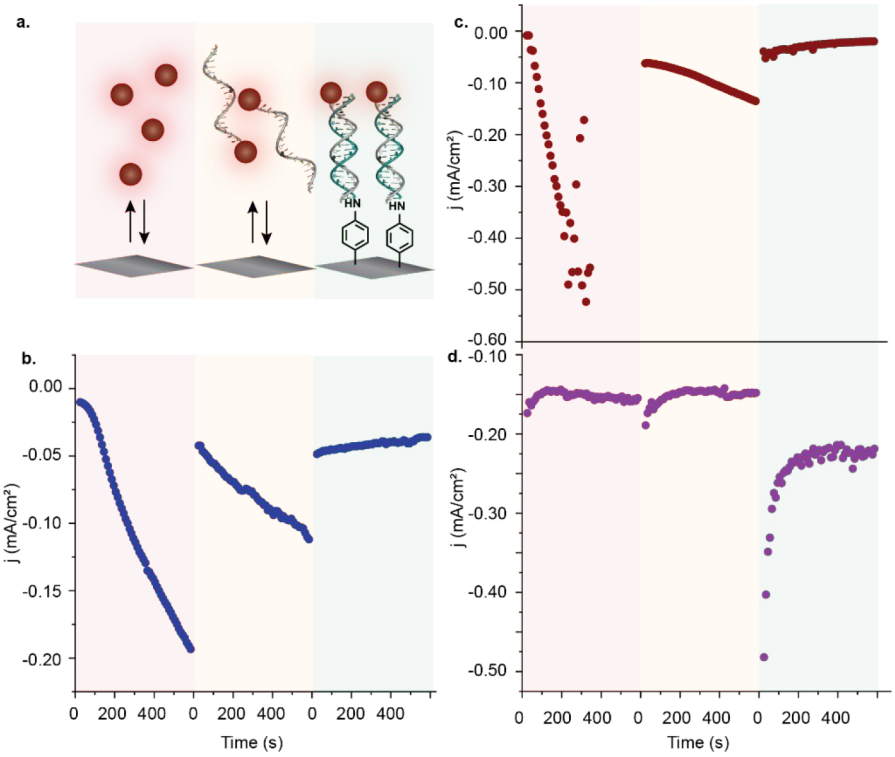

Figure 3. Stability comparison between the free catalyst, ssDNA-modified catalyst, and dsDNA immobilized catalyst. (a) Schematic of catalysts. (b–d) Chronoamperometry of catalysts (CoTCPP: blue, FeTCPP: red, or Hemin: purple) in the three conditions at −1.2 V vs SHE. Experiments were performed on carbon SPEs, and the electrolyte used is KCl (0.1 M) and K_2CO_3 (0.5 M) at pH 7.4, adjusted by adding aliquots of HCl.

aniline-modified carbon paper, the surface coverage of oligonucleotides was calculated to be 147 pmol/cm^2 (the geometric surface area of carbon paper) by RuHex DNA quantification. Confirmation of consistent carbon electrode modification with DNA, especially because low-cost SPEs and carbon paper electrodes were used in this study, is essential to the success of immobilization of electrocatalysts on electrodes.

DNA Hybridization Efficiency

Having successfully modified SPEs with ssDNA, we next examined DNA hybridization or "Velcro" efficiency with respect to ssDNA-modified surfaces. Both DNA-modified electrodes and complementary DNA-catalyst conjugates were heated to 65 °C. The ssDNA-catalyst conjugate was added to the complementary DNA-modified electrode. The electrode was then slowly cooled to room temperature over 1 h, and the unbound catalyst-DNA conjugates were removed by repeated washing. Hybridization efficiency of the ssDNA electrode surface was evaluated by RuHex DNA quantification.

Impressively, the total charge obtained by integration of the redox peaks in the CVs was calculated to be 1.64 μC after catalyst-DNA hybridization, whereas the total charge from the ssDNA-modified SPE was determined to be 0.84 μC (Figure 2b). Thus, the surface density of the catalyst is estimated to be 6.4 pmol/cm^2, achieving near-unity hybridization efficiency (the surface concentration of single-strand oligonucleotides on the SPE surface was calculated to be 6.5 pmol/cm^2; detailed methods for quantification are described in the SI). Moreover, in the presence of CO_2, a 10-fold increase in current was observed by chronoamperometry for the catalyst-modified electrode in KCl/K_2CO_3 electrolyte as compared to the electrode modified only with ssDNA. These data indicate that the catalyst-DNA was successfully immobilized on the electrode through DNA hybridization and that the hybridization maintained the activity of the catalyst (Figure S9). This observation is important for the application of DNA hybridization at an electrode for catalysis, as altering the activity or accessibility of biomolecules on surfaces is often a concern following immobilization.

Stability of Catalysts under Relevant Electrochemical Conditions

Though TCPP-based catalysts have been established for many energy-relevant transformations, one key challenge with their implementation is their instability. These and catalysts with similar ligand structures are prone to deactivation.[64−66] Indeed, both CoTCPP and FeTCPP at −1.2 V vs SHE (the potential at which the CO_2RR occurs) show rapid decomposition. The significant change in current indicates that catalyst decomposition and, potentially, precipitation onto the electrode occur in this electrochemical potential regime (Figure 3). Despite the instability of the TCPP catalysts, the current observed by chronoamperometry for hemin remains stable at −1.2 V vs SHE. Taken together, our chronoamperometry stability data confirm our observations for the ssDNA modification of these catalysts. When these homogeneous molecular catalysts are in solution, they are unstable at the requisite potential for the CO_2RR, making them unsuitable for this conversion at scale.

The challenges in optimizing coupling conditions highlight one of the key drawbacks of porphyrin derivatives: their limited solubility in aqueous buffers. Surprisingly, though, following DNA modification, we observed an interesting phenomenon: a significant improvement in the aqueous solubility of the catalysts. Thus, though our ultimate goal was to immobilize these catalysts on electrodes using DNA "Velcro", we took a step back to investigate the impact of DNA

https://doi.org/10.1021/jacsau.3c00823
JACS Au 2024, 4, 1413−1421

addition to the catalysts in solution. We evaluated the stability of the conjugates as well as their ability to perform the CO_2RR, without immobilization to the electrode. When compared to the largely insoluble small-molecule catalysts, the DNA conjugates were found to be highly soluble in aqueous buffers without the addition of cosolvents. This is a significant finding, as fully aqueous-soluble catalysts allow for additional flexibility in the pH and buffering conditions as well as the electrolyte that can be used with the system. Both of these variables significantly impact CO_2RR efficiency independent of the catalyst, making the ability to tune these parameters without solubility concerns a significant advantage of our strategy.[67] Given our results, we anticipate that a range of energy-relevant conversions could be improved through the catalyst modification with DNA.

The DNA-modified hemin demonstrated similar stability to the unmodified version, which is unsurprising, as the catalyst was stable in the absence of the ssDNA. Interestingly, the addition of DNA to the TCPP-derived catalysts provided an immediate and significant improvement in catalyst stability. Under the same electrochemical conditions as were used to evaluate the unmodified porphyrin catalysts, the DNA-modified catalysts maintained their activity and remained stable at potentials that caused degradation for the small-molecule catalysts alone (Figure S10). Thus, simply adding the soluble oligonucleotide significantly improved the stability of the catalysts in solution (Figure 3). Although solvent effects are established for CO_2RR catalysis, this finding supports the impact of the local environment of the metal center on the stability of the small molecules, beyond simple pH and ionic effects. The next step was therefore to tackle the overall efficiency of catalysis, which we anticipated would be improved through the application of DNA "Velcro" to immobilize the catalysts on electrodes.

Surprisingly, for DNA-immobilized CoTCPP, steady currents were observed by chronoamperometry at lower overpotentials (−0.95 V vs SHE), indicating that DNA "Velcro" leads to improved CO_2RR catalyst stability (Figure S11). Both FeTCPP and hemin immobilized with DNA showed stable currents at relevant potentials for CO_2RR (−1.2 V vs SHE), despite their homogeneous equivalents showing degradation at this potential (Figure 3). Impressively, the amount of CO generated from the pm/cm^2 of the catalyst immobilized on the electrode is comparable to the amount generated from μM concentrations of the homogeneous catalyst in solution (Figure S12). The observation of CO by gas chromatography (GC) confirms that the catalyst center remains the active site on the electrode, as no CO production was observed for DNA-modified electrodes alone (Figure S13).

CO_2RR in Solution with Porphyrin-Based Catalysts

We initially investigated CO_2RR of these three porphyrin-derived catalysts in solution using SPEs in aqueous carbonate electrolyte because of their prevalence in CO_2RR studies.[68−70] Additionally, the free porphyrin-based catalysts are soluble in this class of solvents at the concentrations used herein. As seen in Figure 4, catalytic current is observed by cyclic voltammetry (CV) using 0.5 mM CoTCPP in an aqueous carbonate electrolyte saturated with CO_2 at neutral pH. In the absence of CO_2, the observed current was threefold lower than in its presence (−1.2 V vs SHE, Figure 4a). Similarly, the current generated by FeTCPP under the same conditions exhibited a

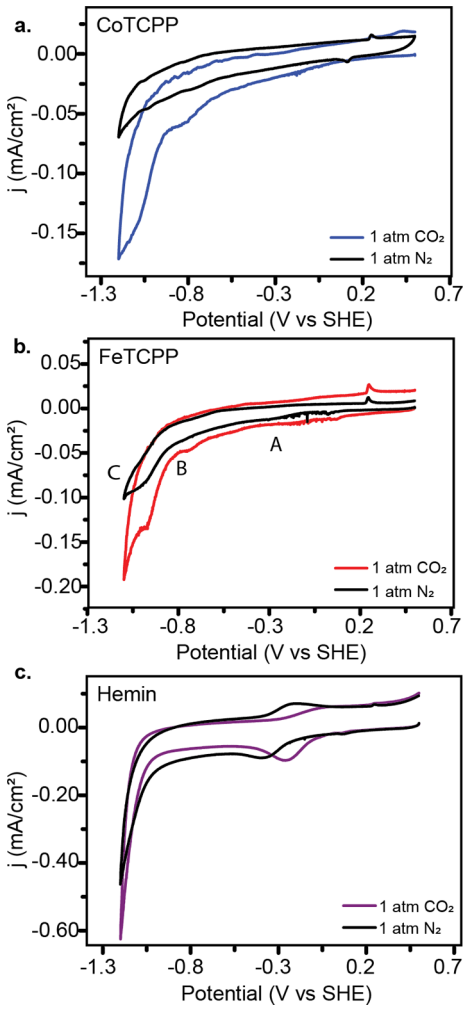

Figure 4. Homogeneous electrochemical CO_2 reduction in aqueous buffers. (a−c) Cyclic voltammetry (CV) of CoTCPP, FeTCPP or Hemin (0.5 mM total concentration), under nitrogen (black) and CO_2 (colored), carried out at a scan rate of 100 mVs^{-1}, on screen-printed electrodes. The electrolyte used is KCl (0.1 M) and K_2CO_3 (0.5 M) at pH 7.4, adjusted by adding aliquots of HCl.

twofold increase when the buffer was saturated with CO_2. Under a N_2 atmosphere, three redox processes are observed. Peak A is attributed to the $Fe^{III/II}$ couple, while peaks B and C are attributed to the irreversible $Fe^{II/I}$ reduction and hydrogen evolution, respectively, which is supported by prior literature characterization.[71−73] The increase in current observed in the $Fe^{I/0}$ potential region (between −1.2 and −1.1 V vs SHE) when CO_2 is present in the solution is indicative of CO_2RR, which was later confirmed by GC.

In contrast to the TCPP-based catalysts, no significant difference in current was observed for 0.5 mM hemin in a 95% buffer/5% acetonitrile (ACN) solution in the presence or absence of CO_2 (Figure 4c). The addition of ACN to the solvent for this catalyst is due to its limited solubility in aqueous electrolyte alone. The observation of equivalent current generation is explained by the inevitable competition between the reduction of CO_2 and hydrogen evolution in aqueous buffers. Indeed, the results from the chromatographic analysis of the gaseous products generated in the headspace of the electrochemical cell indicate that the CO production rates are relatively low with this catalyst (Figure S12).

https://doi.org/10.1021/jacsau.3c00823
JACS Au 2024, 4, 1413−1421

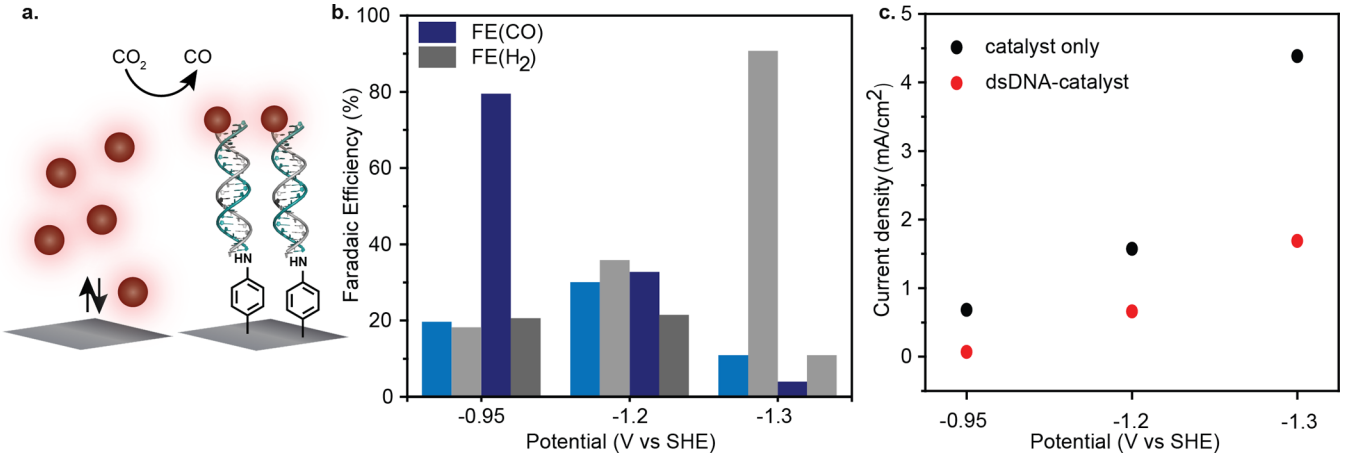

Figure 5. DNA-modified electrochemistry in solution and on an electrode. (a) Schematic representation of free catalyst or DNA-modified catalyst hybridized onto the carbon paper surface. (b,c) In-line gas chromatography (GC) analysis. (b) Faradaic efficiencies toward CO and H_2 at different applied potentials using free catalyst (light blue, light gray) and DNA-immobilized catalysts (dark blue, dark gray) on carbon paper (CO_2 flow rate: 10 sccm), carried out at −0.95, −1.2, and −1.3 V vs SHE; and (c) total current densities at different applied potentials using free catalyst (black) and DNA-immobilized catalyst (red). The electrolyte used is KCl (0.1 M) and K_2CO_3 (0.5 M) at pH 7.4, adjusted by adding aliquots of HCl.

In order to accurately determine the efficiency of porphyrin-based small-molecule catalysts for CO_2RR in aqueous buffer, we tested CoTCPP in a customized two-compartment cell separated by an ion-exchange membrane to prevent platinum (Pt) crossover. A carbon paper working electrode and Pt foil counter electrode are used with this cell (Figure S14). Using an in-line GC, the FEs toward CO for CoTCPP-based catalysts were calculated to be 19.6, 30.0, and 10.9% at −0.95, −1.2, and −1.3 V vs SHE (Figures 5, S14 and S18a), respectively. Thus, these bioinspired small-molecule catalysts are capable of CO_2RR, but their efficiency is too low for broad utility. Further, the concentrations required for catalysis (often mM) are inefficient, making them unsuitable for larger-scale systems.

Electrocatalysis Improvements

Owing to low surface area of carbon SPEs, the products of CO_2RR from the dsDNA-catalyst-modified electrodes are relatively low compared to the competing hydrogen evolution reaction based on our results from in-line GC. To accurately determine the FE of the system, dsDNA-catalyst-modified carbon paper was tested as the working electrode in the custom cell (Figure S14, detail in the Supporting Information). The CoTCPP-ssDNA conjugates were hybridized to the surface of carbon paper modified with complementary ssDNA. After RuHex quantification of the DNA on the surface was compared to the catalyst electrochemical signal (Figure S16), the surface density of the catalyst was estimated to be 144 pmol/cm^2 (geometric surface area of carbon paper), demonstrating a hybridization efficiency of over 98% (the surface concentration of single-strand oligonucleotides on carbon paper was calculated to be 147 pmol/cm^2, as described previously). For CoTCPP immobilized with DNA, CO_2 electrocatalysis was observed at a less negative overpotential (−0.95 V vs SHE), and high selectivity toward CO formation was observed by GC with minimal hydrogen evolution (Figure S15). The FE of CoTCPP immobilized with DNA toward CO is calculated to be 79.1%. This efficiency represents a fourfold increase compared to the homogeneous molecular catalysts (19.6%) (Figures 5, S14, S15 and S20). When applying a higher overpotential (−1.2 V vs SHE), the FE(CO) of the heterogeneous system is 32.7%, higher than that of the homogeneous system (30.0%). As expected, the hydrogen evolution competing reaction dominated for both systems when they were held at a more negative potential (−1.3 V vs SHE). The immobilization of ssDNA-catalyst conjugates on electrodes had the intended effect: improving FE while maintaining the improved stability observed with ssDNA-catalyst conjugates in solution.

Furthermore, we evaluated the buffer effect on the selectivity of the CO_2RR using catalyst-dsDNA-modified carbon paper. The sodium bicarbonate electrolyte at neutral pH has the highest selectivity toward CO relative to H_2 formation (Figure S17). Taken together, these results demonstrate the circumvention of key challenges in the CO_2RR with small-molecule catalysts: stability and efficiency. Finally, we measured the turnover frequency (TOF) for each of the three catalysts under each DNA modification condition. For each catalyst, the free, small-molecule catalyst, the ssDNA-catalyst, and the DNA-immobilized catalyst are compared. As can be seen in Figure 6, DNA-immobilized catalysts yielded TOFs at least an order of magnitude (for CoTCPP) and as high as 3 orders of magnitude (for FeTCPP and hemin) higher than free catalysts in solution. Thus, not only does the addition of DNA improve the stability and FE of the system, but also DNA-immobilized catalyst demonstrates significantly higher turnover rates.

The elegance of enzymatic reactions has inspired the integration of biomolecules such as amino acids and peptides with CO_2RR catalysis to improve selectivity and solubility.[20,74,75] In this study, we evaluated the ability of DNA to serve as a molecular "Velcro" to tether porphyrin-based small-molecule CO_2RR catalysts to electrodes. For the metalloporphyrin catalysts employed in this study, the efficiency of the CO_2RR for the desired CO product is closely related to the microenvironment surrounding the metal centers. We theorize that the improved CO_2RR efficiency observed in our system is due to alterations in the outer coordination sphere resulting from the presence of DNA. Moreover, we observed that, for DNA-immobilized CoTCPP, CO_2RR could be carried out at a lower overpotential than for homogeneous catalysis (−0.95 V vs SHE), which is likely due to the increased stability and solvent accessibility of the catalyst.

Overall, we have demonstrated that DNA "Velcro" to tether catalysts to electrodes improves their efficiency and stability.

https://doi.org/10.1021/jacsau.3c00823
JACS Au 2024, 4, 1413−1421

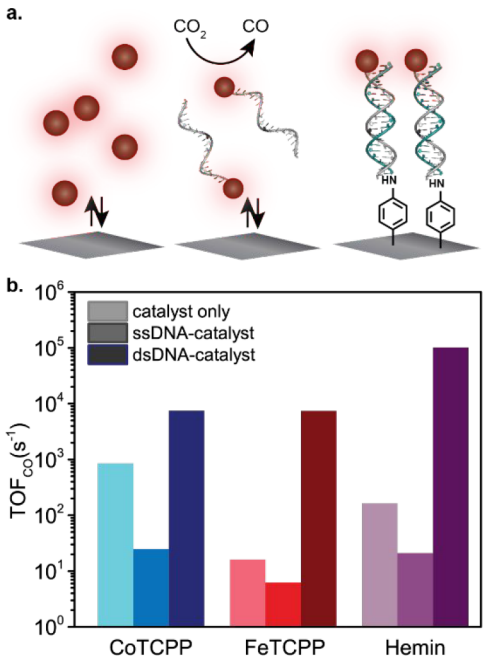

Figure 6. Turnover frequency (TOF) measurements for the three porphyrin catalysts studied. (a) For each catalyst, free small-molecule catalyst (left), ssDNA-catalyst (center), and DNA-immobilized catalyst (right) were evaluated. (b) TOFs for CO production by each catalyst were measured by comparing current densities to in-line quantified CO. The electrolyte used is KCl (0.1 M) and K_2CO_3 (0.5 M) at pH 7.4, adjusted by adding aliquots of HCl.

The readily-synthesized catalyst-ssDNA conjugates afford improved aqueous solubility. Furthermore, the DNA hybridization-based CO_2RR catalyst immobilization yielded systems with higher TOF compared to the unmodified controls. Taken together, our results provide an important proof-of-principle demonstration of the power of DNA "Velcro" to improve catalysis. We anticipate that this platform will be a powerful tool to enable the increased activity and stability of many additional important classes of catalysts.

MATERIALS AND METHODS

Functionalization of Amino-Modified DNAs with Metalated TCPP Catalysts by the HATU/DIPEA Method

In a typical reaction, to a solution of amino-modified DNA (2.0 nmol) in MOPS buffer (300 μL, 50 mM, 0.5 M NaCl, pH 8.0) was added a mixture of FeTCPP (0.2 mg, 240 nmol), HATU (0.8 mg, 2.1 μmol), and DIPEA (0.4 μL, 2.1 μmol) in 300 μL of DMF at room temperature. The reaction was agitated for 24 h and resulted in covalent attachment of the FeTCPP complex to the DNA. The DNA-catalyst conjugates were then purified by reverse-phase HPLC using a water (50 mM TEAA) (solvent A)/ACN (solvent B) gradient and characterized by MALDI-TOF mass spectrometry.

ASSOCIATED CONTENT

Supporting Information

The Supporting Information is available free of charge at https://pubs.acs.org/doi/10.1021/jacsau.3c00823.

Chemicals and reagents; analysis and measurement; metal complex, DNA-catalyst, and DNA-aminophenol conjugates synthesis; carbon electrode modification; quantitation of surface-attached ssDNA using hexaammineruthenium (III) trichloride (RuHex); catalyst immobilization by DNA hybridization; CO_2 reduction product measurements; MALDI-TOF MS analysis; UV−vis spectra of single-stranded DNA 1; RP-HPLC trace of purified FeTCPP-ssDNA, CoTCPP-ssDNA, and hemin-ssDNA; *p*-nitroaniline was used to modified glass carbon electrode; oxidative coupling reaction; voltammetry of free and immobilized catalysts; cyclic voltammograms of the three catalysts; and stability of catalyst (PDF)

AUTHOR INFORMATION

Corresponding Author

Ariel L. Furst − *Department of Chemical Engineering, Massachusetts Institute of Technology, Cambridge, Massachusetts 02139, United States; Center for Environmental Health Sciences, Massachusetts Institute of Technology, Cambridge, Massachusetts 02139, United States;* orcid.org/0000-0001-9583-9703; Email: afurst@mit.edu

Authors

Gang Fan − *Department of Chemical Engineering, Massachusetts Institute of Technology, Cambridge, Massachusetts 02139, United States;* orcid.org/0000-0002-4185-5692

Nathan Corbin − *Department of Chemical Engineering, Massachusetts Institute of Technology, Cambridge, Massachusetts 02139, United States*

Minju Chung − *Department of Chemical Engineering, Massachusetts Institute of Technology, Cambridge, Massachusetts 02139, United States;* orcid.org/0000-0003-4359-7508

Thomas M. Gill − *Department of Chemical Engineering, Massachusetts Institute of Technology, Cambridge, Massachusetts 02139, United States*

Evan B. Moore − *Department of Chemical Engineering, Massachusetts Institute of Technology, Cambridge, Massachusetts 02139, United States*

Amruta A. Karbelkar − *Department of Chemical Engineering, Massachusetts Institute of Technology, Cambridge, Massachusetts 02139, United States*

Complete contact information is available at: https://pubs.acs.org/10.1021/jacsau.3c00823

Author Contributions

[§]M.C. and T.M.G. contributed equally.

Notes

The authors declare no competing financial interest.

ACKNOWLEDGMENTS

We acknowledge the Army Research Office (W911NF- 22-1-0106), the CIFAR Azrieli Global Scholars Program, the MIT Energy Initiative, and the MIT Deshpande Center for funding this work. N.C. was funded by a grant from the National Science Foundation (no. 1955628).

REFERENCES

(1) Aresta, M.; Dibenedetto, A. Utilisation of CO2 as a Chemical Feedstock: Opportunities and Challenges. *Dalton Transactions* **2007**, *28*, 2975−2992.

(2) Koytsoumpa, E. I.; Bergins, C.; Kakaras, E. The CO2 Economy: Review of CO2 Capture and Reuse Technologies. *J. Supercrit. Fluids* **2018**, *132*, 3−16.
(3) Salimijazi, F.; Kim, J.; Schmitz, A. M.; Grenville, R.; Bocarsly, A.; Barstow, B. Constraints on the Efficiency of Engineered Electromicrobial Production. *Joule* **2020**, *4*, 2101.
(4) Heidlage, M. G.; Kezar, E. A.; Snow, K. C.; Pfromm, P. H. Thermochemical Synthesis of Ammonia and Syngas from Natural Gas at Atmospheric Pressure. *Ind. Eng. Chem. Res.* **2017**, *56* (47), 14014−14024.
(5) Dry, M. E. The Fischer−Tropsch Process: 1950−2000. *Catal. Today* **2002**, *71* (3), 227−241.
(6) Dry, M. E. Practical and Theoretical Aspects of the Catalytic Fischer−Tropsch Process. *Appl. Catal. A Gen* **1996**, *138* (2), 319−344.
(7) Abdulaeva, I. A.; Birin, K. P.; Michalak, J.; Romieu, A.; Stern, C.; Bessmertnykh-Lemeune, A.; Guilard, R.; Gorbunova, Y. G.; Tsivadze, A. Yu. On the Synthesis of Functionalized Porphyrins and Porphyrin Conjugates via *β*-Aminoporphyrins. *New J. Chem.* **2016**, *40* (7), 5758−5774.
(8) Corbin, N.; Zeng, J.; Williams, K.; Manthiram, K. Heterogeneous Molecular Catalysts for Electrocatalytic CO2 Reduction. *Nano Res.* **2019**, *12* (9), 2093−2125.
(9) Benson, E. E.; Kubiak, C. P.; Sathrum, A. J.; Smieja, J. M. Electrocatalytic and Homogeneous Approaches to Conversion of CO2 to Liquid Fuels. *Chem. Soc. Rev.* **2009**, *38* (1), 89−99.
(10) Nielsen, D. U.; Hu, X.-M.; Daasbjerg, K.; Skrydstrup, T. Chemically and Electrochemically Catalysed Conversion of CO2 to CO with Follow-up Utilization to Value-Added Chemicals. *Nat. Catal* **2018**, *1* (4), 244−254.
(11) Hori, Y.; Murata, A.; Kikuchi, K.; Suzuki, S. Electrochemical Reduction of Carbon Dioxides to Carbon Monoxide at a Gold Electrode in Aqueous Potassium Hydrogen Carbonate. *J. Chem. Soc. Chem. Commun.* **1987**, *10*, 728−729.
(12) Liu, Y.; Leung, K. Y.; Michaud, S. E.; Soucy, T. L.; McCrory, C. C. L. Controlled Substrate Transport to Electrocatalyst Active Sites for Enhanced Selectivity in the Carbon Dioxide Reduction Reaction. *Comments on Inorganic Chemistry* **2019**, *39* (5), 242−269.
(13) Kramer, W. W.; McCrory, C. C. L. Polymer Coordination Promotes Selective CO2 Reduction by Cobalt Phthalocyanine. *Chem. Sci.* **2016**, *7* (4), 2506−2515.
(14) Oh, S.; Gallagher, J. R.; Miller, J. T.; Surendranath, Y. Graphite-Conjugated Rhenium Catalysts for Carbon Dioxide Reduction. *J. Am. Chem. Soc.* **2016**, *138* (6), 1820−1823.
(15) Hu, X.-M.; Rønne, M. H.; Pedersen, S. U.; Skrydstrup, T.; Daasbjerg, K. Enhanced Catalytic Activity of Cobalt Porphyrin in CO2 Electroreduction upon Immobilization on Carbon Materials. *Angew. Chem., Int. Ed.* **2017**, *56* (23), 6468−6472.
(16) Austin, N.; Zhao, S.; McKone, J. R.; Jin, R.; Mpourmpakis, G. Elucidating the Active Sites for CO2 Electroreduction on Ligand-Protected Au25 Nanoclusters. *Catal. Sci. Technol.* **2018**, *8* (15), 3795−3805.
(17) Chen, K.; Arnold, F. H. Engineering New Catalytic Activities in Enzymes. *Nat. Catal* **2020**, *3* (3), 203−213.
(18) Chen, J. G.; Crooks, R. M.; Seefeldt, L. C.; Bren, K. L.; Bullock, R. M.; Darensbourg, M. Y.; Holland, P. L.; Hoffman, B.; Janik, M. J.; Jones, A. K.; Kanatzidis, M. G.; King, P.; Lancaster, K. M.; Lymar, S. V.; Pfromm, P.; Schneider, W. F.; Schrock, R. R. Beyond Fossil Fuel−Driven Nitrogen Transformations. *Science (1979)* **2018**, *360* (6391), No. eaar6611.
(19) Le, J. M.; Bren, K. L. Engineered Enzymes and Bioinspired Catalysts for Energy Conversion. *ACS Energy Lett.* **2019**, *4* (9), 2168−2180.
(20) Fan, G.; Wasuwanich, P.; Furst, A. L. Biohybrid Systems for Improved Bioinspired, Energy-Relevant Catalysis. *ChemBioChem.* **2021**, *22*, 2353.
(21) Prier, C. K.; Arnold, F. H. Chemomimetic Biocatalysis: Exploiting the Synthetic Potential of Cofactor-Dependent Enzymes To Create New Catalysts. *J. Am. Chem. Soc.* **2015**, *137* (44), 13992−14006.
(22) Elgrishi, N.; Griveau, S.; Chambers, M. B.; Bedioui, F.; Fontecave, M. Versatile Functionalization of Carbon Electrodes with a Polypyridine Ligand: Metallation and Electrocatalytic H+ and CO2 Reduction. *Chem. Commun.* **2015**, *51* (14), 2995−2998.
(23) Atoguchi, T.; Aramata, A.; Kazusaka, A.; Enyo, M. Electrocatalytic Activity of CoII TPP-Pyridine Complex Modified Carbon Electrode for CO2 Reduction. *J. Electroanal Chem. Interfacial Electrochem* **1991**, *318* (1), 309−320.
(24) Atoguchi, T.; Aramata, A.; Kazusaka, A.; Enyo, M. Cobalt(II)−Tetraphenylporphyrin−Pyridine Complex Fixed on a Glassy Carbon Electrode and Its Prominent Catalytic Activity for Reduction of Carbon Dioxide. *J. Chem. Soc. Chem. Commun.* **1991**, *3*, 156−157.
(25) Tanaka, H.; Aramata, A. Aminopyridyl Cation Radical Method for Bridging between Metal Complex and Glassy Carbon: Cobalt(II) Tetraphenylporphyrin Bonded on Glassy Carbon for Enhancement of CO2 Electroreduction. *J. Electroanal. Chem.* **1997**, *437* (1), 29−35.
(26) Mohamed, E. A.; Zahran, Z. N.; Naruta, Y. Efficient Heterogeneous CO2 to CO Conversion with a Phosphonic Acid Fabricated Cofacial Iron Porphyrin Dimer. *Chem. Mater.* **2017**, *29* (17), 7140−7150.
(27) Blakemore, J. D.; Gupta, A.; Warren, J. J.; Brunschwig, B. S.; Gray, H. B. Noncovalent Immobilization of Electrocatalysts on Carbon Electrodes for Fuel Production. *J. Am. Chem. Soc.* **2013**, *135* (49), 18288−18291.
(28) Kang, P.; Zhang, S.; Meyer, T. J.; Brookhart, M. Rapid Selective Electrocatalytic Reduction of Carbon Dioxide to Formate by an Iridium Pincer Catalyst Immobilized on Carbon Nanotube Electrodes. *Angew. Chem., Int. Ed.* **2014**, *53* (33), 8709−8713.
(29) Maurin, A.; Robert, M. Noncovalent Immobilization of a Molecular Iron-Based Electrocatalyst on Carbon Electrodes for Selective, Efficient CO2-to-CO Conversion in Water. *J. Am. Chem. Soc.* **2016**, *138* (8), 2492−2495.
(30) Kornienko, N.; Zhao, Y.; Kley, C. S.; Zhu, C.; Kim, D.; Lin, S.; Chang, C. J.; Yaghi, O. M.; Yang, P. Metal−Organic Frameworks for Electrocatalytic Reduction of Carbon Dioxide. *J. Am. Chem. Soc.* **2015**, *137* (44), 14129−14135.
(31) Palla, K. S.; Hurlburt, T. J.; Buyanin, A. M.; Somorjai, G. A.; Francis, M. B. Site-Selective Oxidative Coupling Reactions for the Attachment of Enzymes to Glass Surfaces through DNA-Directed Immobilization. *J. Am. Chem. Soc.* **2017**, *139* (5), 1967−1974.
(32) Faraone-Mennella, J.; Tezcan, F. A.; Gray, H. B.; Winkler, J. R. Stability and Folding Kinetics of Structurally Characterized Cytochrome C-B562. *Biochemistry* **2006**, *45* (35), 10504−10511.
(33) Chidchob, P.; Edwardson, T. G. W.; Serpell, C. J.; Sleiman, H. F. Synergy of Two Assembly Languages in DNA Nanostructures: Self-Assembly of Sequence-Defined Polymers on DNA Cages. *J. Am. Chem. Soc.* **2016**, *138* (13), 4416−4425.
(34) Jones, M. R.; Seeman, N. C.; Mirkin, C. A. Programmable Materials and the Nature of the DNA Bond. *Science (1979)* **2015**, *347* (6224), 1260901.
(35) Hamblin, G. D.; Hariri, A. A.; Carneiro, K. M. M.; Lau, K. L.; Cosa, G.; Sleiman, H. F. Simple Design for DNA Nanotubes from a Minimal Set of Unmodified Strands: Rapid, Room-Temperature Assembly and Readily Tunable Structure. *ACS Nano* **2013**, *7* (4), 3022−3028.
(36) Macfarlane, R. J.; Jones, M. R.; Senesi, A. J.; Young, K. L.; Lee, B.; Wu, J.; Mirkin, C. A. Establishing the Design Rules for DNA-Mediated Programmable Colloidal Crystallization. *Angew. Chem., Int. Ed.* **2010**, *49* (27), 4589−4592.
(37) Wang, P.; Meyer, T. A.; Pan, V.; Dutta, P. K.; Ke, Y. The Beauty and Utility of DNA Origami. *Chem.* **2017**, *2* (3), 359−382.
(38) Aldaye, F. A.; Sleiman, H. F. Modular Access to Structurally Switchable 3D Discrete DNA Assemblies. *J. Am. Chem. Soc.* **2007**, *129* (44), 13376−13377.
(39) McLaughlin, C. K.; Hamblin, G. D.; Sleiman, H. F. Supramolecular DNA Assembly. *Chem. Soc. Rev.* **2011**, *40* (12), 5647−5656.

https://doi.org/10.1021/jacsau.3c00823
JACS Au 2024, 4, 1413−1421

(40) Buchberger, A.; Simmons, C. R.; Fahmi, N. E.; Freeman, R.; Stephanopoulos, N. Hierarchical Assembly of Nucleic Acid/Coiled-Coil Peptide Nanostructures. *J. Am. Chem. Soc.* **2020**, *142* (3), 1406−1416.
(41) Furst, A. L.; Smith, M. J.; Lee, M. C.; Francis, M. B. DNA Hybridization To Interface Current-Producing Cells with Electrode Surfaces. *ACS Cent Sci.* **2018**, *4* (7), 880−884.
(42) Furst, A.; Landefeld, S.; Hill, M. G.; Barton, J. K. Electrochemical Patterning and Detection of DNA Arrays on a Two-Electrode Platform. *J. Am. Chem. Soc.* **2013**, *135* (51), 19099−19102.
(43) Nano, A.; Furst, A. L.; Hill, M. G.; Barton, J. K. DNA Electrochemistry: Charge-Transport Pathways through DNA Films on Gold. *J. Am. Chem. Soc.* **2021**, *143*, 11631.
(44) Boal, A. K.; Barton, J. K. Electrochemical Detection of Lesions in DNA. *Bioconjug Chem.* **2005**, *16* (2), 312−321.
(45) Furst, A. L.; Barton, J. K. DNA Electrochemistry Shows DNMT1Methyltransferase Hyperactivity in Colorectal Tumors. *Chem. Biol.* **2015**, *22* (7), 938−945.
(46) Furst, A. L.; Muren, N. B.; Hill, M. G.; Barton, J. K. Label-Free Electrochemical Detection of Human Methyltransferase from Tumors. *Proc. Natl. Acad. Sci. U. S. A.* **2014**, *111* (42), 14985−14989.
(47) Douglas, E. S.; Chandra, R. A.; Bertozzi, C. R.; Mathies, R. A.; Francis, M. B. Self-Assembled Cellular Microarrays Patterned Using DNA Barcodes. *Lab Chip* **2007**, *7* (11), 1442−1448.
(48) Furst, A. L.; Klass, S. H.; Francis, M. B. DNA Hybridization to Control Cellular Interactions. *Trends Biochem. Sci.* **2019**, *44* (4), 342−350.
(49) Hsiao, S. C.; Shum, B. J.; Onoe, H.; Douglas, E. S.; Gartner, Z. J.; Mathies, R. A.; Bertozzi, C. R.; Francis, M. B. Direct Cell Surface Modification with DNA for the Capture of Primary Cells and the Investigation of Myotube Formation on Defined Patterns. *Langmuir* **2009**, *25* (12), 6985−6991.
(50) Douglas, E. S.; Hsiao, S. C.; Onoe, H.; Bertozzi, C. R.; Francis, M. B.; Mathies, R. A. DNA-Barcode Directed Capture and Electrochemical Metabolic Analysis of Single Mammalian Cells on a Microelectrode Array. *Lab Chip* **2009**, *9* (14), 2010−2015.
(51) Twite, A. A.; Hsiao, S. C.; Onoe, H.; Mathies, R. A.; Francis, M. B. Direct Attachment of Microbial Organisms to Material Surfaces through Sequence-Specific DNA Hybridization. *Adv. Mater.* **2012**, *24* (18), 2380−2385.
(52) Fukuzumi, S.; Lee, Y. M.; Ahn, H. S.; Nam, W. Mechanisms of Catalytic Reduction of CO2 with Heme and Nonheme Metal Complexes. *Chem. Sci.* **2018**, *9* (28), 6017−6034.
(53) Calzadiaz-Ramirez, L.; Meyer, A. S. Formate Dehydrogenases for CO2 Utilization. *Curr. Opin Biotechnol* **2022**, *73*, 95−100.
(54) Alpdağtaş, S.; Turunen, O.; Valjakka, J.; Binay, B. The Challenges of Using NAD+-Dependent Formate Dehydrogenases for CO2 Conversion. *Crit Rev. Biotechnol* **2022**, *42* (6), 953−972.
(55) Sørensen, M.; Andersen-Ranberg, J.; Hankamer, B.; Møller, B. L. Circular Biomanufacturing through Harvesting Solar Energy and CO_2. *Trends Plant Sci.* **2022**, *27* (7), 655−673.
(56) Casas, C.; Lacey, C. J.; Meunier, B. Preparation of Hybrid "DNA Cleaver-Oligonucleotide" Molecules Based on a Metallotris (Methylpyridiniumyl)Porphyrin Motif. *Bioconjug Chem.* **1993**, *4* (5), 366−371.
(57) Boutorine, A. S.; Brault, D.; Takasugi, M.; Delgado, O.; Hélène, C. Chlorin-Oligonucleotide Conjugates: Synthesis, Properties, and Red Light-Induced Photochemical Sequence-Specific DNA Cleavage in Duplexes and Triplexes. *J. Am. Chem. Soc.* **1996**, *118* (40), 9469−9476.
(58) Stulz, E. Nanoarchitectonics with Porphyrin Functionalized DNA. *Acc. Chem. Res.* **2017**, *50* (4), 823−831.
(59) Llamas, E. M.; Tome, J. P. C.; Rodrigues, J. M. M.; Torres, T.; Madder, A. Porphyrin-Based Photosensitizers and Their DNA Conjugates for Singlet Oxygen Induced Nucleic Acid Interstrand Crosslinking. *Org. Biomol Chem.* **2017**, *15* (25), 5402−5409.
(60) Li, Y.; Gabriele, E.; Samain, F.; Favalli, N.; Sladojevich, F.; Scheuermann, J.; Neri, D. Optimized Reaction Conditions for Amide Bond Formation in DNA-Encoded Combinatorial Libraries. *ACS Comb. Sci.* **2016**, *18* (8), 438−443.
(61) Karbelkar, A.; Ahlmark, R.; Fan, G.; Yang, V.; Furst, A. Oxidative Coupling for Facile, Stable Carbon Modification with DNA and Proteins. *ChemRxiv* **2022**.
(62) Yu, H. Z.; Luo, C. Y.; Sankar, C. G.; Sen, D. Voltammetric Procedure for Examining DNA-Modified Surfaces: Quantitation, Cationic Binding Activity, and Electron-Transfer Kinetics. *Anal. Chem.* **2003**, *75* (15), 3902−3907.
(63) Furst, A.; Hill, M. G.; Barton, J. K. Electrocatalysis in DNA Sensors. *Polyhedron* **2014**, *84*, 150−159.
(64) Shu, Y.; Liu, X.; Zhang, M.; Liu, B.; Wang, Z. Deactivation of Porphyrin Metal-Organic Framework in Advanced Oxidation Process: Photobleaching and Underlying Mechanism. *Applied Catalysis B: Environment and Energy* **2024**, *346*, 123746.
(65) Cai, Z.; Huang, M.; Dai, J.; Zhan, G.; Sun, F.; Zhuang, G.-L.; Wang, Y.; Tian, P.; Chen, B.; Ullah, S.; Huang, J.; Li, Q. Fabrication of Pd/In2O3 Nanocatalysts Derived from MIL-68(In) Loaded with Molecular Metalloporphyrin (TCPP(Pd)) Toward CO2 Hydrogenation to Methanol. *ACS Catal.* **2022**, *12* (1), 709−723.
(66) Yabuki, R.; Nishimura, K.; Hamachi, T.; Matsumoto, N.; Yanai, N. Generation and Transfer of Triplet Electron Spin Polarization at the Solid−Liquid Interface. *J. Phys. Chem. Lett.* **2023**, *14* (20), 4754−4759.
(67) Costentin, C.; Robert, M.; Savéant, J. M.; Tatin, A. Efficient and Selective Molecular Catalyst for the CO2-to-CO Electrochemical Conversion in Water. *Proc. Natl. Acad. Sci. U. S. A.* **2015**, *112* (22), 6882−6886.
(68) Zhu, M.; Ye, R.; Jin, K.; Lazouski, N.; Manthiram, K. Elucidating the Reactivity and Mechanism of CO2 Electroreduction at Highly Dispersed Cobalt Phthalocyanine. *ACS Energy Lett.* **2018**, *3* (6), 1381−1386.
(69) Torbensen, K.; Han, C.; Boudy, B.; von Wolff, N.; Bertail, C.; Braun, W.; Robert, M. Iron Porphyrin Allows Fast and Selective Electrocatalytic Conversion of CO_2 to CO in a Flow Cell. *Chem. − Eur. J.* **2020**, *26* (14), 3034−3038.
(70) Walsh, J. J.; Neri, G.; Smith, C. L.; Cowan, A. J. Water-Soluble Manganese Complex for Selective Electrocatalytic CO2 Reduction to CO. *Organometallics* **2019**, *38* (6), 1224−1229.
(71) Bhugun, I.; Lexa, D.; Savéant, J.-M. Catalysis of the Electrochemical Reduction of Carbon Dioxide by Iron(0) Porphyrins. Synergistic Effect of Lewis Acid Cations. *J. Phys. Chem.* **1996**, *100* (51), 19981−19985.
(72) Costentin, C.; Drouet, S.; Robert, M.; Savéant, J.-M. A Local Proton Source Enhances CO2 Electroreduction to CO by a Molecular Fe Catalyst. *Science (1979)* **2012**, *338* (6103), 90−94.
(73) Bhugun, I.; Lexa, D.; Saveant, J.-M. Ultraefficient Selective Homogeneous Catalysis of the Electrochemical Reduction of Carbon Dioxide by an Iron(0) Porphyrin Associated with a Weak Broensted Acid Cocatalyst. *J. Am. Chem. Soc.* **1994**, *116* (11), 5015−5016.
(74) Chabolla, S. A.; MacHan, C. W.; Yin, J.; Dellamary, E. A.; Sahu, S.; Gianneschi, N. C.; Gilson, M. K.; Tezcan, F. A.; Kubiak, C. P. Bio-Inspired CO2 Reduction by a Rhenium Tricarbonyl Bipyridine-Based Catalyst Appended to Amino Acids and Peptidic Platforms: Incorporating Proton Relays and Hydrogen-Bonding Functional Groups. *Faraday Discuss.* **2017**, *198* (c), 279−300.
(75) Walsh, A. P.; Laureanti, J. A.; Katipamula, S.; Chambers, G. M.; Priyadarshani, N.; Lense, S.; Bays, J. T.; Linehan, J. C.; Shaw, W. J. Evaluating the Impacts of Amino Acids in the Second and Outer Coordination Spheres of Rh-Bis(Diphosphine) Complexes for CO2 Hydrogenation. *Faraday Discuss.* **2019**, *215*, 123−140.

https://doi.org/10.1021/jacsau.3c00823
JACS Au 2024, 4, 1413−1421